Direct Measurement of Solvation Forces in Complex Microporous Media: A New Characterization Tool

Josh Samuel,[†] C. Jeffrey Brinker,[‡,§] Laura J. Douglas Frink,*[,||] and Frank van Swol[§,⊥]

Satec Ecochem, P.O. Box 45022 Jerusalem 91450, Israel, Direct Fabrication Department, 1831, Sandia National Laboratories, Albuquerque, New Mexico 87185-1349, UNM/NSF Center for Micro-Engineered Materials, University of New Mexico, Albuquerque, New Mexico 87131, Computational Materials Science Department 9225, Sandia National Laboratories, Albuquerque, New Mexico 87185-1111, and Theoretical and Computational Materials Modeling Department 1841, Sandia National Laboratories, Albuquerque, New Mexico 87185-1349

Received January 15, 1998. In Final Form: March 24, 1998

We present a new beam bending (BB) technique for measuring solvation forces in complex microporous materials. The solvation forces are compressive and monotonically increasing with relative pressure. This is in stark contrast to Laplace−Kelvin theory (LKT) which predicts only tensile stresses. Applying a nonlocal density functional theory (DFT), the observed monotonic, compressive stresses are shown to arise from molecular sized pores with modest pore size polydispersity where the half-width of the distribution is 0.2−0.7 nm. Finally, the combined BB/DFT analysis provides a novel and much needed method for characterizing the morphology of microporous thin film materials to 0.1 nm resolution.

Solvation forces arising in confined fluids,[1] including capillary drying stress,[2] electrostatic interactions,[3] and short-range oscillatory forces,[4] are influential in a wide range of natural processes and advanced technologies. While these forces have previously been measured in what are essentially single idealized pores with the surface forces apparatus (SFA),[4] little is known about how these forces (in particular the short-range oscillatory forces) act in complex porous materials. We confine our discussion to microporous thin films used for membranes, sensors, and catalysts; however, the short-range forces that dictate the response of these thin films also act between macromolecules in solution and therefore play an important (although poorly understood) role in controlling the interactions and state of assembly of many macromolecular systems including proteins, polymers, and micelles.[5,6]

The beam bending apparatus (BBA) we describe here is detailed in the inset of Figure 1, and measures the response of a porous film to changes in the vapor content of the surrounding atmosphere. Sol−gel processing is used to deposit a microporous silica film on one side of a thin single crystal ⟨100⟩ silicon wafer.[7] After the film is calcined to 500 °C to stabilize the microporous silica structure, the wafer is suspended vertically in a vacuum system, and the microporous film is equilibrated with the vapor of a sorbate.[8] The change in substrate curvature is measured as a function of relative pressure of the vapor. The measured (macroscopic) bending stress S_{bend} is derived from the small lateral deflection of the wafer using Stoney's equation.[8] Provided that the stresses in the solid network of the porous material change very little with adsorption, the BBA measures changes in the solvent induced forces (or solvation forces) in the porous network.

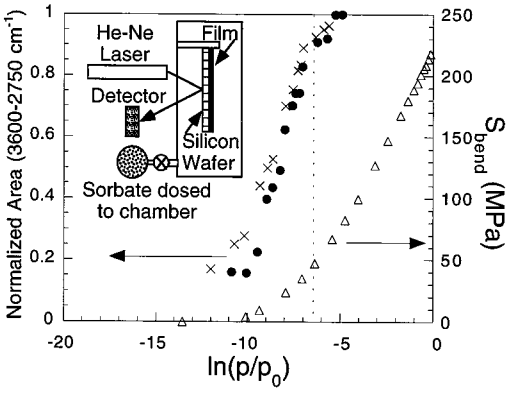

Figure 1. Stress and adsorption isotherms measured for A2 films exposed to methanol vapor. The various symbols are as follows: ×, adsorption; ●, desorption; and △, stress. Arrows point to the appropriate axes. The dotted line indicates the approximate relative pressure at which the film is saturated. Inset: Schematic of the BBA. A silicon wafer coated with a microporous silica film is fixed at one end in a vacuum chamber thus forming a cantilever. A He−Ne laser is reflected off the uncoated side of the wafer, and the height of the reflected spot is monitored. The reflection of the laser is related to the lateral deflection of the cantilever caused by solvation forces in the film. The film thickness was ≈1000 Å.

In a single pore, the solvation force per unit area, f_s, is defined as $f_s = p_{pore} - p$, where p_{pore} is the pressure acting

[†] Satec Ecochem.

[‡] Direct Fabrication Department, 1831, Sandia National Laboratories.

[§] University of New Mexico.

[||] Computational Materials Science Department, 9225, Sandia National Laboratories.

[⊥] Theoretical and Computational Materials Modeling Department, Sandia National Laboratories.

(1) Evans, R.; Marini Bettolo Marconi, U. *J. Chem. Phys.* **1987**, *86*, 7138.

(2) Scherer, G. W. *J. Am. Ceram. Soc.* **1990**, *73*, 3.

(3) Tang, Z.; Scriven, L. E.; Davis, H. T. *J. Chem. Phys.* **1994**, *100*, 4527.

(4) Horn, R. G.; Israelachvili, J. N. *J. Chem. Phys.* **1981**, *75*, 1400. *Appl. Phys. Lett.* **1992**, *60*, 2356.

(5) Rau, D. C.; Parsegian, V. A. *Biophys. J.* **1992**, *61*, 260.

(6) Frink, L. J. D.; van Swol, F. *J. Chem. Phys.* **1994**, *100*, 9106.

(7) Brinker, C. J.; Ward, T. L.; Sehegal, R.; Raman, N. K.; Hietala, S. L.; Smith, D. M.; Hua, D.-W.; Headly, T. J. *J. Membr. Sci.* **1993**, *77*, 165.

(8) Voncken, J. H. L.; Lijzenga, C.; Kumar, K. P.; Keizer, K.; Burggraaf, A. J.; Bonekamp, B. C. *J. Mater. Sci.* **1992**, *27*, 472.

S0743-7463(98)00073-0 CCC: $15.00
Published on Web 04/22/1998

on the inside of the pore walls and p is the bulk pressure in the surrounding atmosphere.[1] For a random porous medium filled with a dense (e.g. capillary condensed) fluid, the bending stress is linked to the mean solvation force, $\langle f_s \rangle$, acting on the film[7,9] via

$$S_{\text{bend}} = (1 - 2\eta)(1 - K_n/K_s)/(1 - \eta)\langle f_s \rangle = \alpha \langle f_s \rangle \quad (1)$$

where η is Poisson's ratio of the film, and K_n and K_s are the bulk moduli of the film and silica skeleton respectively. The proportionality constant, α, depends on the particular film and substrate in the experiment. However, using accepted literature values for the material parameters, α is always in the range $\alpha = 0.4-1$ and can be determined to within 20%.[7]

A typical experiment measures S_{bend} (or the solvation force relative to $\langle f_s(p = 0) \rangle = 0$) as a function of the relative pressure of the solvent in the vapor phase, thus yielding a *stress isotherm*. Adsorption, desorption, and bending stress isotherms for methanol in a microporous silica film (A2) with pore radius of 0.32 nm are shown in Figure 1. The mean pore radius is established by a size exclusion experiment where sorbate molecules of differing size are introduced into the vacuum chamber. The largest molecule to fit into the pores and the smallest molecule to be excluded from the pores are determined by whether or not a stress response is obtained for a particular sorbate. For A2 films, ethanol is the largest sorbate that caused a deflection of the BBA cantilever. With 2-propanol there was no response.

The adsorption isotherm in Figure 1 was determined by transmission FTIR spectroscopy. The isotherm is very sharp, and adsorption is essentially complete at $\ln(p/p_o) = -6.5 (p/p_o = 0.0015)$. A TEM micrograph of the film was featureless when viewed at magnifications that clearly resolved the 2 nm pore radius of an underlying γ-Al_2O_3 support.[9] The exclusion of 2-propanol, the sharp Type I isotherm, and the fine texture of the silica film from TEM are all consistent with molecular-sized (<1 nm in diameter) pores.[10]

The stress isotherm in Figure 1 shows that S_{bend} increases monotonically with relative pressure, reaching 220 MPa ($\langle f_s \rangle \approx 450$ MPa, $\alpha = 0.48$, eq 1) at saturation ($p/p_o = 1$). While the adsorption primarily occurs at $p/p_o < 0.0015$, most of the stress change occurs at higher relative pressures where the pores are filled with condensed fluid. Hence, unlike clay systems, which swell tremendously with adsorption,[11,12] the majority of the stress develops in our films with very little change in pore volume. We estimate that the pore dimensions only change by 0.00004%.[13]

Figure 2 compares the dimensionless solvation force isotherms for a series of adsorbates in both the A2 films and a microporous silica film (P-25) prepared with higher porosity and a larger average pore radius of 0.43 nm.[14] In all cases, a monotonic compressive stress is observed. The slopes taken with respect to $\ln(p/p_o)$ at saturation are found

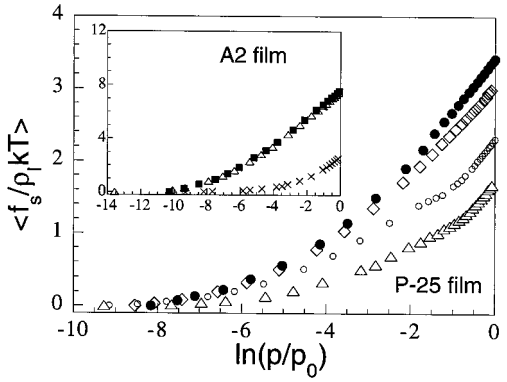

Figure 2. The mean solvation force in a P-25 film ($\alpha \approx 1.0$) normalized by the liquid density of the sorbate, ρ_l, as a function of the relative pressure for a series of sorbates (●) *tert*-butyl alcohol; (◇) 2-propanol; (○) ethanol; (△) methanol. Inset: Solvation force in an A2 film ($\alpha \approx 0.48$) for (●) methanol, (△) *n*-acetonitrile, and (×) water.

to be equal within 20% to $kT\rho_l$ where k is the Boltzmann constant, T is the absolute temperature, and ρ_l is the number density of bulk liquid at coexistence.

Of course, Laplace−Kelvin theory (LKT), which assumes that the fluid in the pores has a *uniform* density of ρ_l,[1] also predicts a slope of $kT\rho_l$. The solvation force in LKT is

$$f_s(p,T) = \begin{cases} kT\rho_l (\cos\theta)[\ln(p/p_o)]; & p_t < p < p_o \\ 0 & \text{otherwise} \end{cases} \quad (2)$$

where p_t is the pressure at which capillary condensation occurs, θ is the contact angle, and the vapor is assumed to be an ideal gas. If the fluid completely wets the porous material (as is the case here), $\cos\theta = 1$, and LKT predicts that $\partial f_s/\partial(\ln(p/p_o)) = kT\rho_l$.

While LKT correctly predicts the slope observed with the BBA, it does not predict the observed compressive stresses. On the contrary, LKT predicts only tensile stresses in pores containing capillary condensed fluids. This particular failing of LKT arises from the assumption of a uniform pore fluid.

Modern molecular theories,[1] molecular simulation,[15] and experiments[4] have all demonstrated that fluids confined in pores of molecular size exhibit density oscillations that reflect packing constraints. Since all the evidence indicates that LKT should fail when applied to microporous materials, it is very surprising that LKT correctly predicts the slope of the BBA stress isotherms. The challenge thus lies in developing a theoretical approach to properly treat the packing effects that are known to exist in small pores while reproducing the LKT slope at saturation. Without such a molecular approach, it would be impossible to reconcile SFA results (namely oscillatory forces) with those of the BBA.

In order to analyze the BBA results, we have applied a nonlocal DFT that can capture solvent packing effects.[16] In our model the porous network is assumed to be composed of independent smooth slits with some polydispersity in pore size.[17] The fluid−fluid and fluid−wall interactions are taken to be 12−6 and 9−3 Lennard−Jones potentials, respectively. All the potentials are cut and shifted to zero at 10σ where σ is the solvent diameter.

(9) Brinker, C. J.; Scherer, G. W. *Sol-Gel Science*; Academic Press: San Diego, CA, 1990.
(10) Everett, D. H. IUPAC Manual of Symbols and Terminology. *Pure Appl. Chem.* **1972**, *31*, 578.
(11) Smalley, M. V.; Thomas, R. K.; Braganza, L. F.; Matsuo, T. *Clays Clay Miner.* **1989**, *37*, 474.
(12) Douglas, L. J.; Lupkowski, M.; Dodd, T.; van Swol, F. *Langmuir* **1993**, *9*, 1442.
(13) For a BBA stress of 250 MPa, the in-plane dimensional change of the film deposited on a 5 cm beam is 20 nm corresponding to an in plane strain of 4×10^{-7}.
(14) Raman, N. K.; Brinker, C. J. *J. Membr. Sci.* **1995**, *105*, 273.
(15) Snook, I.; van Megen, W. *J. Chem. Phys.* **1979**, *70*, 3099.
(16) Rosenfeld, Y. *Phys. Rev. Lett.* **1989**, *63*, 980; *J. Chem. Phys.* **1993**, *98*, 8120.
(17) Alternatively one can interpret non-uniformity in the films in terms of surface roughness within the pores. See: Douglas Frink, L. J.; van Swol, F. *J. Chem. Phys.* **1998**, *108*, 5588.

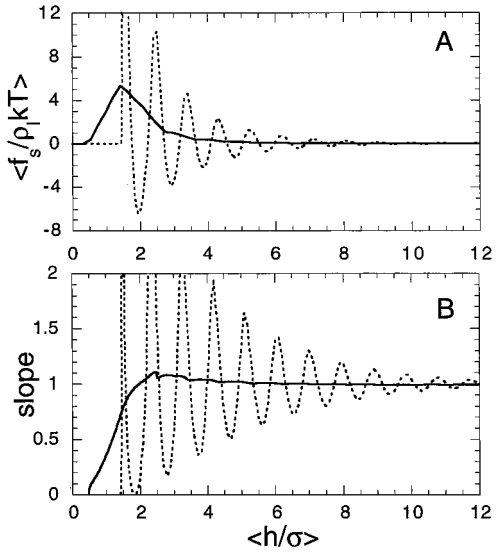

Figure 3. (A) Mean solvation force, $\langle f_s \rangle$, and (B) derivative of $\langle f_s \rangle$ with respect to $\ln(p/p_o)$ (slope $= \partial\langle f_s/\rho_l kT\rangle/\partial(\ln(p/p_o))$) as a function of pore size for a Lennard−Jones fluid in a network of slit pores. The bulk vapor state point corresponds to a bulk fluid near saturation close to the triple point temperature. The reduced temperature is $kT/\epsilon = 0.74$. The dashed lines detail the single pore (or monodisperse network) result. The solid lines detail the result for a polydisperse network characterized by $t^* = 0.5$. For $kT/\epsilon = 0.74$, $\rho_l\sigma^3 = 0.82$.

The ratio of the fluid−wall to fluid−fluid interaction potential energy parameter was chosen to be $\epsilon_{wf}/\epsilon = 5$ where $\theta = 0°$.[18] The pore size polydispersity is modeled as a Gaussian distribution about the mean pore size, $\bar{h}$, with a standard deviation of the distribution, t, which is at most on the order of the size of a solvent molecule; i.e., $0 < t^* \equiv t/\sigma < 1$.

We begin by considering the solvation force and the slope as a function of pore size at saturation. Figure 3A shows the variation of the mean solvation force, $\langle f_s/\rho_l kT\rangle$, with the mean pore size, $\bar{h}^* \equiv \bar{h}/\sigma$, for both a single pore (a monodisperse network) and for a polydisperse network where $t^* = 0.5$. Oscillatory forces are predicted for the monodisperse case as expected from SFA measurements.[4] The solvation oscillations are damped as t is increased from $t^* = 0$ leaving a residual positive force for $h^* \leq 4$ at $t^* = 0.5$. The slope of the stress with respect to $\ln(p/p_o)$ at saturation is shown in Figure 3B. The oscillations are nearly symmetric about the LKT slope for the monodisperse case. As a result, the LKT slope is obtained within 20% for all pores with $h^* \geq 1.5$ for $t^* = 0.5$.

The symmetry of the DFT slope about the LKT prediction could not have been guessed in advance. However, this symmetry is crucial in order to obtain the universal observation of this slope in BBA experiments.

The broad positive peak in the force at saturation implies a compressive stress measured at saturation in the BBA. The DFT demonstrates that the consistent observation of these compressive stresses arises from polydispersity on a molecular length scale ($t^* < 1$). If the films were composed of smooth monodisperse pores, Figure 3 shows that it would be only fortuitous to observe both a compressive stress and the LKT slope at saturation, since the LKT slope is only found for select discrete pore sizes. At the other extreme, as the polydispersity becomes large ($t^* >> 1$), we find that the compressive stress is reduced in magnitude (see the trend in Figure 4 at saturation),

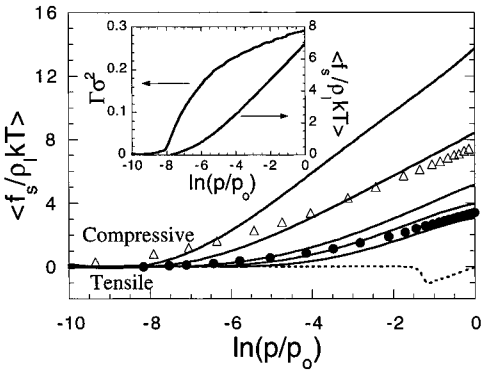

Figure 4. Lines show the mean solvation force as a function of $\ln(p/p_o)$ from DFT for various model polydisperse pore networks. In the solid lines, the mean pore size is $\bar{h}^* = 1.6$, and the curves differ in the degree of polydispersity in the films: from top to bottom, we show $t^* = 0.2$, 0.3, 0.5, 0.7, and 1.0. The dashed line corresponds to a polydisperse network ($t^* = 0.3$) with a larger mean pore size ($\bar{h}^* \approx 6.72$). Symbols show solvation forces from the BBA: (●) *tert*-butyl alcohol in the P-25 film; (△) methanol in the A2 film. Inset: Solvation force and excess adsorption.

and ultimately would vanish. This strong sensitivity of the force to small changes in polydispersity may be exploited to determine the properties of the microporous film.

We now turn to the variation of the solvation force with relative pressure for a fixed mean pore size of $\bar{h}^* = 1.6$. Figure 4 shows the solvation force vs relative pressure for polydispersities $t^* = 0.2-1.0$. In addition, the result for a larger mean pore size ($\bar{h}^* = 6.72$, $t^* = 0.3$) is shown. The smaller pores all show monotonic compressive forces and a limiting LKT slope to within between 15% ($t^* = 0.5$ and 0.7) and 30% ($t^* = 0.2$) error. We note that the large pore exhibits LKT tensile stresses as well as the LKT slope and demonstrates that the DFT obtains the correct limiting behavior.

Comparing Figure 4 with Figures 1 and 2, we see that all the salient features of the BBA results (stresses, the LKT slope at saturation, and well-separated adsorption and stress isotherms) are captured by the DFT of a polydisperse porous network. Furthermore, the DFT predicts that the solvation stress is remarkably sensitive to the degree of polydispersity in the film (see Figure 4).

One way to effectively vary the polydispersity in a given film is to expose that film to adsorbates that differ in size.[19] Increasing polydispersity corresponds to decreasing adsorbate size. The alcohols in Figure 2 (P-25 film) serve as an example. The magnitude of the stress when normalized by ρ_l decreases in the order: *tert*-butyl alcohol to methanol (compare with DFT in Figure 4). Fitting the DFT predictions to the measured stress at saturation, h and t are found to be $\bar{h} = 0.62 \pm 0.11$ nm and $t = 0.196 \pm 0.006$ nm for the A2 film, and $\bar{h} = 0.980 \pm 0.32$ nm and $t = 0.67 \pm 0.05$ nm for the P-25 film. These estimates are in good agreement with the size exclusion experiments which gave pore diameters of 0.64 nm for the A2 film and 0.86 nm for the P-25 film.

In summary, the beam bending technique is a new tool for measuring short-range solvation forces in complex porous films. While other methods (SFA and AFM) may be used to determine solvation forces in a single well-defined pore, the BBA provides insight to the response of

(18) van Swol, F.; Henderson, J. R. *Phys. Rev. A* **1989**, *40*, 2567; **1991**, *43*, 2932.

(19) The normalized mean pore size ($\bar{h}^*$) also changes when molecules of different size (σ) are sorbed into a microporous thin film with fixed pore size (h), but this is a smaller effect.

a complex porous network to those solvation forces. DFT offers a molecular interpretation of the BBA that links the film properties (i.e., the pore size polydispersity) to the measured stress isotherms. Most importantly, we find that the stress response of microporous films is highly sensitive to the degree of polydispersity in pore size. Thus the combined BBA/DFT tool provides a powerful new approach for directly characterizing the pore morphology of thin film specimens, crucially necessary to the development of membranes, sensors, and catalysts.

Acknowledgment. We would like to thank Hong-Bin Yan and Tom Niemczyk for help with the IR measurements, and Richard Cairncross and Alan Hurd for helpful discussions. This work was supported by the United States Department of Energy under Contract DE-AC04-94AL8500. Sandia is a multiprogram laboratory operated by Sandia Corporation, a Lockheed Martin Company, for the United States Department of Energy.

LA980073K